Supplementary Information

Harnessing subcellular-resolved organ distribution of cationic copolymer-functionalized fluorescent nanodiamonds for optimal delivery of active siRNA to a xenografted tumor in mice

*Sandra Claveau, Marek Kindermann, Alexandre Papine, Zamira V. Díaz-Riascos, Xavier Délen, Patrick Georges, Roser López-Alemany, Òscar Martínez Tirado, Jean-Rémi Bertrand, Ibane Abasolo, Petr Cigler, and François Treussart**

Table S1. Characterization of the colloidal properties of batch #1 of Cop$^+$-FND and Cop$^+$-FND:siAS complexes with a mass ratio 25:1 using DLS and ELS. Two first rows, all columns: mean ± standard deviation of two measurements. Rows 3 to 5 (complex in specific medium): the size was measured ten times (during approximately 20 min). As indicators of colloidal stability, two values are displayed: 1st / 10th measurements. More detailed information about the measurement conditions can be found in the Experimental section.

	Z-average diameter [nm]	Apparent ζ-potential [mV]	Electrophoretic mobility [µm·cm/V·s]	Conductivity [µS/cm]	Applied voltage [V]
Cop$^+$-FND (nuclease free water, 25 °C)	138.0 ± 1.0	45.8 ± 2.9	3.59 ± 0.23	5.96 ± 0.05	9.5
Cop$^+$-FND:siRNA (siAS) (nuclease free water, 25 °C)	150.9 ± 6.2	38.4 ± 0.8	3.01 ± 0.07	18.30 ± 0.00	5.0
Cop$^+$-FND:siRNA (siAS) (DMEM, 37 °C)	157.9 / aggregated	-	-	-	-
Cop$^+$-FND:siRNA (siAS) (10% FCS, DMEM, 37 °C)	150.4 / 152.9		-	-	-
Cop$^+$-FND:siRNA (siAS) (100% FCS, 37 °C)	229.9 / 287.7	-	-	-	-

Table S2. Ranges of the automatic detection parameters used to identify Cop$^+$-FND in function of the organ considered. These parameters need to be adjusted to each type of organ due to large differences in their autofluorescence intensities.

	Global contrast	Local contrast	Total intensity [counts/350 ms per ROI]	Area [µm^2]		Ratio of intensity between bleaching and acquisition steps	
	min	min	min	min	max	min	max
Lung	1.3	1.2	30	0.25	7.5	0.65	1.25
Heart	0.8	1.27	20	0.4	9	0.75	1.25
Tumor	1.3	1.13	10	0.25	60	0.65	1.25
Liver	1.3	1.2	30	0.25	20	0.65	1.25
Spleen	1.3	1.2	30	0.25	20	0.65	1.25
Kidney	1.3	1.2	30	0.25	20	0.65	1.25

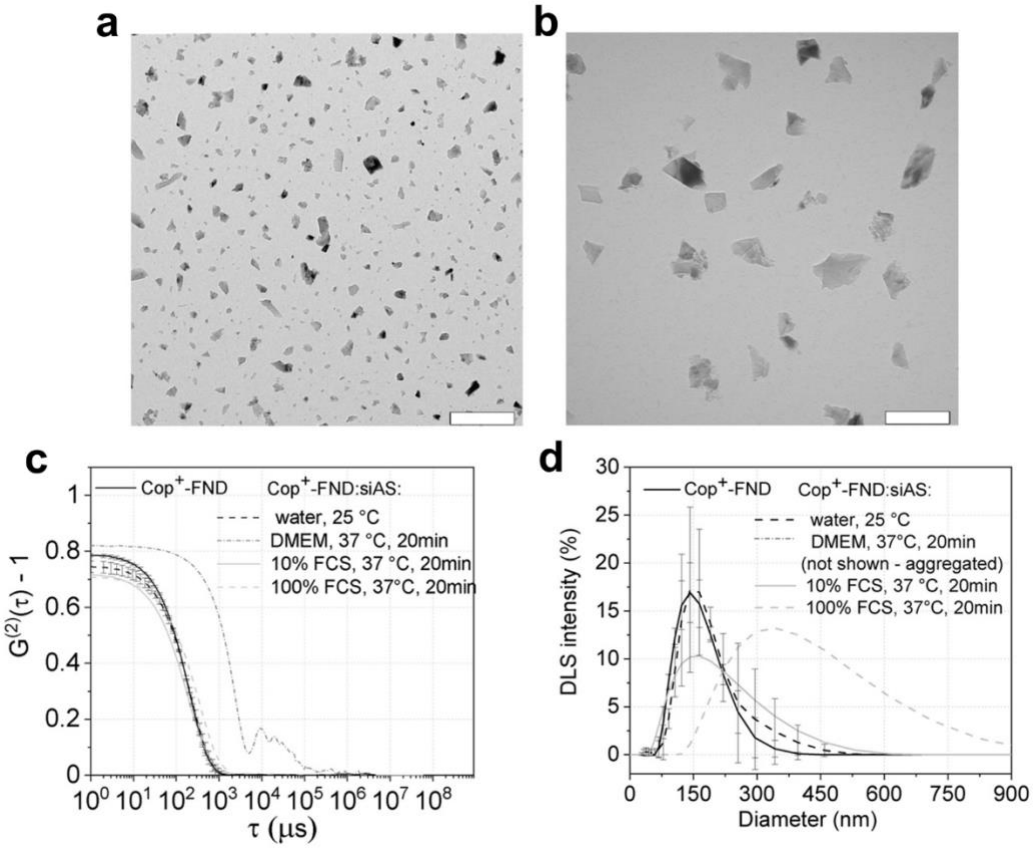

Figure S1. a, b) TEM images of FND samples. a) FND; scale bar: 200 nm. b) Cop$^+$-FND, scale bar:100 nm. The samples were prepared on carbon-coated copper grids. c, d) Size distribution, as measured by DLS, of Cop$^+$-FND and Cop$^+$-FND:siAS of Table S1 samples (mass ratio 25:1). c) Raw DLS time intensity correlation functions $G^{(2)}(\tau)$-1. d) Intensity size distribution as inferred from the correlation data a), using non-negative least square analysis. In water at 25°C (dark grey dashed line) Cop$^+$-FND:siAS size measurement was done twice and we report the average value ± standard deviation. Cop$^+$-FND:siAS in DMEM alone aggregated after 20 min. For Cop$^+$-FND:siAS in DMEM with 10% FCS (conventional cell culture media) and in 100% FCS we display only the 10th measurement (after 20 min).

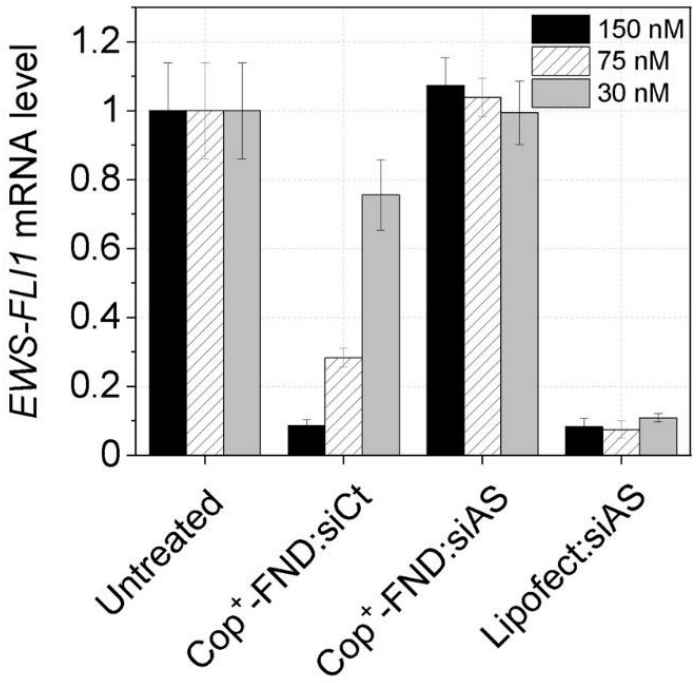

Figure S2. *EWS-FLI1* oncogene inhibition (measured by RT-qPCR) by Cop^{+}-FND complexed with different concentration (30, 75, 150 nM) of siRNA AntiSense (siAS) directed against *EWS-FLI1* junction oncogene or Control (irrelevant siRNA, siCt), and compared to siAS complexed with Lipofectamine 2000 (Lipofect 2000, as a positive control, used without serum added to the medium), at different siRNA concentrations. Cop^{+}-FND:siRNA mass ratio was kept constant and equal to 65:1. mRNA *EWS-FLI1* was extracted 24 h after incubation.

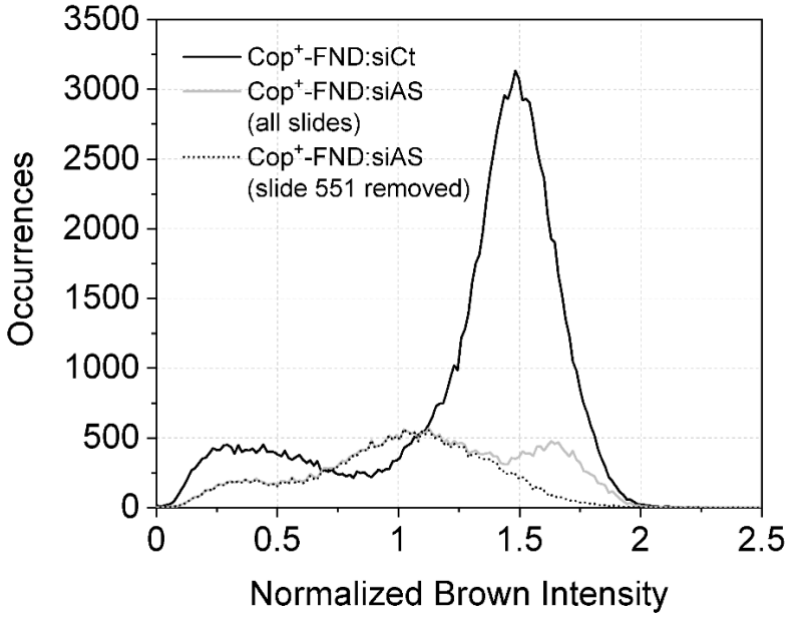

Figure S3. Distributions of EWS-FLI1 immunostaining intensity within individual cell nucleus of tumor region selected by the histopathologist. Two groups are displayed: animals treated by Cop$^+$-FND:siCt (black solid line, data of 4 mice pooled) and Cop$^+$-FND:siAS (grey solid line, data from 5 mice). In the case of Cop$^+$-FND:siAS, the slide histological preparation #551 (1 mice) yielded a high staining intensity, larger than the one of Cop$^+$-FND:Ct, which led us to suspect a labeling issue specific to this sample. After removing this problematic slide (black dashed line, 4 mice) we obtain similar shapes for Cop$^+$-FND:siCt and Cop$^+$-FND:siAS with two peaks, one at low intensity (around 0.3) corresponding to EWS-FLI1 negative labeling and the other one at high intensity (≈1.5 in the case of Cop$^+$-FND:siCt) associated to positive nuclei. Cop$^+$-FND to siRNA mass ratio of 25:1.

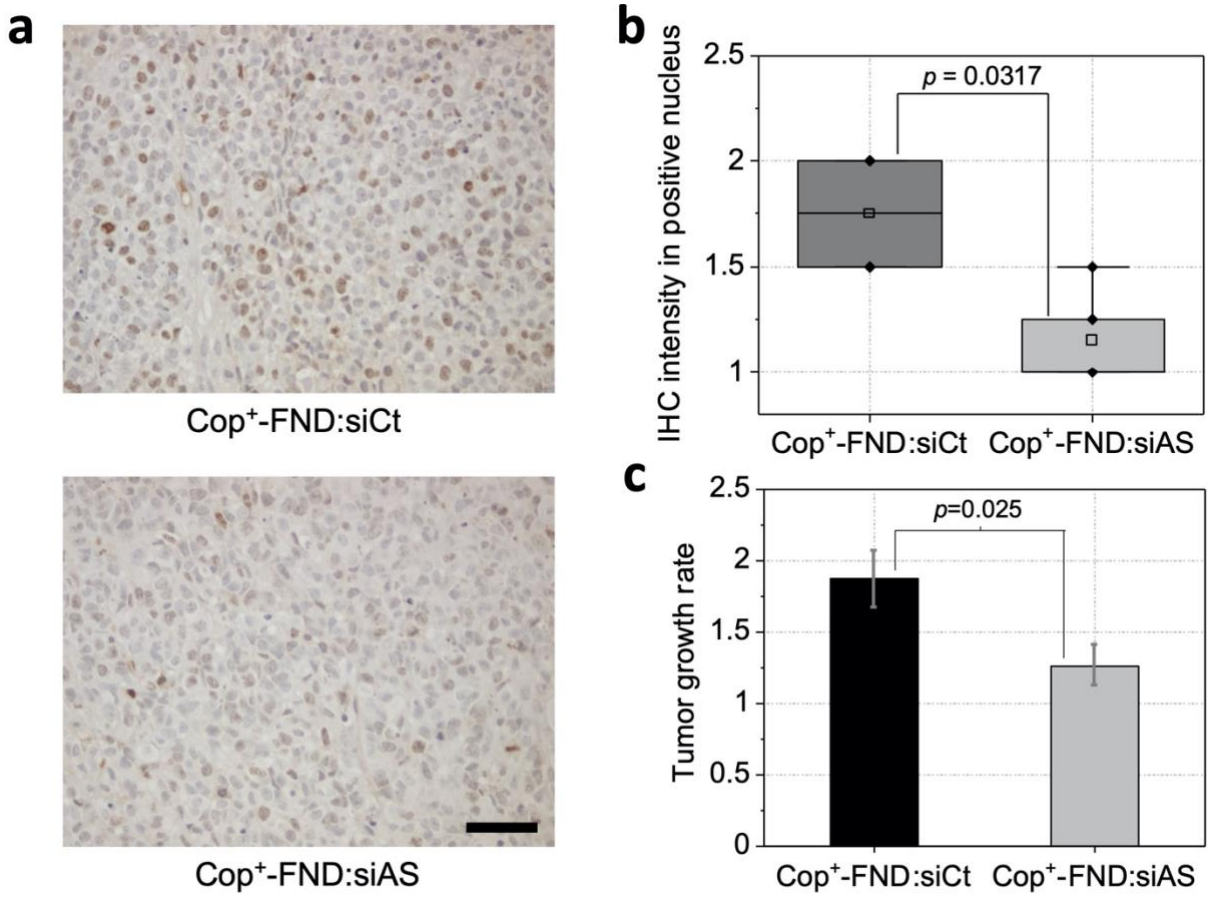

Figure S4. *In vivo* efficacy of Cop+-FND:siRNA in subcutaneous A673 xenografts 48 h after intratumoral administration. Cop+-FND:siRNA mass ratio of 25:1. a) Ki67 IHC in tumors treated with FND with control siRNA (Cop+-FND:siCt) or the siRNA targeting *EWS-FLI1*gene (Cop+-FND:siAS); *n*=4-5 mice per group; scale bar: 50 μm. b) IHC quantification corresponding to the scoring of Ki67 labeling intensity within cell nuclei by two blinded observers and showing statistically significant (p=0.0317, using Wilcoxon-Mann-Whitney test) lower Ki67 content in Cop+-FND:siAS treated sample compared to Cop+-FND:siCt. c) Tumor volume growth rate expressed as the ratio of the final volume to the initial one, 48 h after i.t. administration of Cop+-FND:siRNA. Treatement with siAS yielded a statistically significant (p=0.0255) smaller growth rate than with siCt.

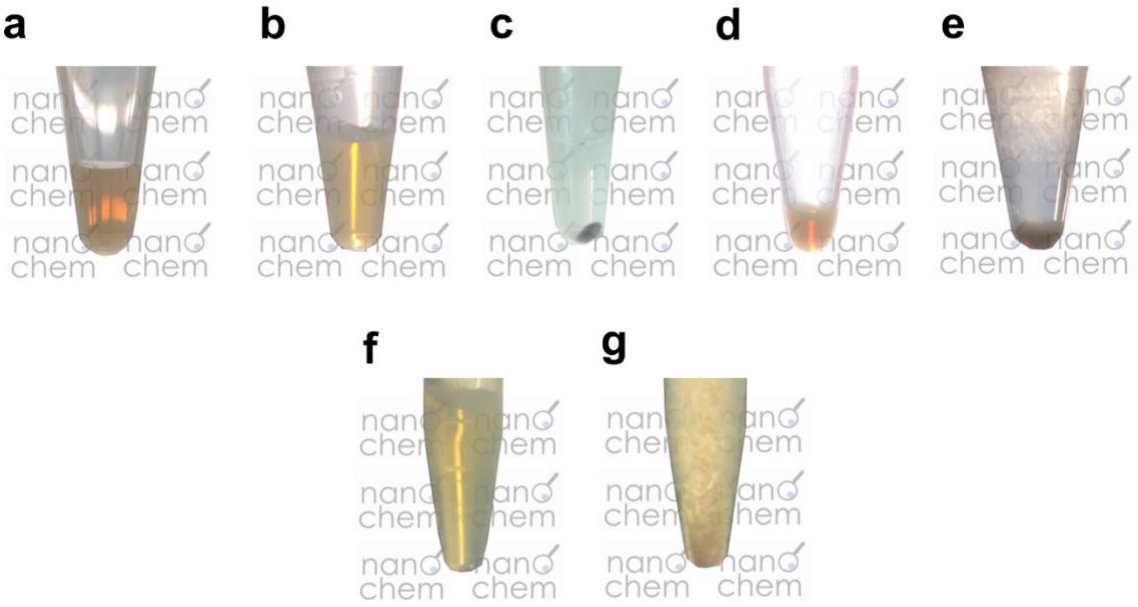

Figure S5. Picture of dispersions of a) Cop^+-FND (8 mg/mL); b) Cop^+-FND:siAS (3.9 mg Cop^+-FND/mL; 0.16 mg siAS/mL; i.e. 750 µg Cop^+-FND/tube; 30 µg siAS/tube); c) Sample (b) after centrifugation (20,000/ min); d) Dissolved sample (c) with the following concentration of components: 12.5 mg Cop^+-FND/mL; 0.5 mg siAS/mL, corresponding to the 25:1 mass ratio; e) Dissolved sample (c) with the following concentration of components: 37.5 mg Cop^+-FND/mL; 1.5 mg siAS/mL; f) FND (2 mg/mL), g) FND-PEI (0.8 kDa, branched) mixture (1:1 v/v; 2 mg FND/mL; 0.9 mg PEI/mL). Samples (a), (b), (d), (f) show the colloidal opalescence characteristic for sample stability. The opalescence of the sample (e) is masked due to high concentration of the complexes. Sample (g) exhibits aggregation which is typical for the mixture of FND and PEI but that can be reversed, resulting back in a transparent colloidal ND-PEI suspension (sample not shown).

***